Finite-frequency optical absorption in 1D conductors and Mott-Hubbard insulators

J. M. P. Carmelo[1,2], N. M. R. Peres [2], and P. D. Sacramento[3]

[1] *CNLS, Los Alamos National Laboratory, Los Alamos, New Mexico 87545*

[2] *Department of Physics, University of Évora, Apartado 94, P-7002-554 Évora, Portugal*

[3] *Departamento de Física and CFIF, IST, Avenida Rovisco Pais, P-1049-001 Lisboa, Portugal*

(Received 5 October 1999)

The frequency-dependent conductivity is studied for the one-dimensional Hubbard model, using a selection rule, the Bethe ansatz, and symmetries associated with conservation laws. For densities where the system is metallic the absorption spectrum has two contributions, a Drude peak at $\omega = 0$ separated by a pseudogap from a broad absorption band whose lower edge is characterized by a non-classical critical exponent. Our findings shed new light on the "far infrared puzzle" and other optical properties of metallic organic chain compounds.

PACS numbers: 72.15. Nj, 05.30. Fk, 72.90.+y, 03.65. Ca

Organic chain materials [1] have a broken symmetry ground state (GS) and at low critical temperatures T_{tr} undergo transitions to unusual $T > T_{tr}$ states. Recent $T > T_{tr}$ optical measurements over a huge frequency range [1,2] established a pseudogap feature together with a zero-frequency mode for the $(TMTSF)_2X$ salts ($TMTSF$ for tetramethyl tetraselena fulvalene.) These experiments have raised several important yet unresolved issues. The first [1] was related to the relevance of calculations based on the doped 1D Hubbard model. Although these materials have finite interchain hopping integrals t_b and t_c with $t_a >> t_b >> t_c$ [1], hopping becomes less effective as the temperature or the frequency is increased and the along-chain hopping t_a dominates.

In this Letter we study the optical conductivity of the 1D Hubbard model, $\sigma_1(\omega) = 2\pi D\delta(\omega) + \sigma_1^{reg}(\omega)$, where $\sigma_1^{reg}(\omega)$ is defined in Eq. (1) below. Schulz [3] used the Bethe-ansatz (BA) solution to calculate D and to derive the total intensity of finite-frequency transitions. Our study refers to all parameter space where that intensity is significant. Analytical calculations of $\sigma_1^{reg}(\omega)$ have so far been restricted to the insulator half filling phase in the limit of large onsite repulsion U [4]. In this case the optical gap occurs at $E_{opt} = U - 4t_a$, followed by an absorption band extending up to $U + 4t_a$ [4,5,6]. Our study confirms the expectation [1] that calculations based on the doped 1D Hubbard model are relevant for the theoretical understanding of recent optical experiments [1,2]. In the metallic phase we find that the finite-frequency transitions are limited to a well-defined band above a pseudogap (which is actually *smallest* at half filling). The occurrence of such pseudogap agrees with predictions from exact diagonalizations which have found practically almost no low-frequency ($\omega \neq 0$) absorption at the metallic phase [7]. By combining symmetries associated with conservation laws [8] with the approach of Ref. [9], we are able to derive the exponent for the frequency dependence above the absorption edge (and below the top edge for half filling). We confirm [1] that the existence of a pseudogap in the charge excitations with the absence of a gap for spin excitations is an indication of charge-spin separation in the metallic state and that that separation is distinct from that of a 1D Tomanaga-Luttinger liquid (TLL), in which both excitations are gapless [1]. We characterize the nature of the

unusual metallic state which following Ref. [1] we call *doped-Mott-Hubbard liquid* (DMHL). Our study reveals that in the case of the 1D Hubbard model previous naive TLL theoretical studies [10] of $\sigma_1^{reg}(\omega)$ do not apply to values of ω larger than the pseudogap. In contrast to previous predictions [2], we find that the phenomenon of suppressed far infrared conductivity is of 1D character and follows from a parity selection rule which also occurs at higher dimensions. However, only at 1D is this selection rule effective in preventing far infrared conductivity transitions. For instance, in the 2D case doping away from half filling induces significant mid-infrared absorption [7,11]. These results seem to indicate that although for low temperatures just above T_{tr} the small interchain coupling might lead to 2D character for some of the properties of the $(TMTSF)_2X$ salts, in what the conductivity along the chains is concerned the main role of that coupling is equivalent to small doping on the single chains, which otherwise remain of 1D character, with the electrons confined in each chain.

The 1D Hubbard model in a chemical potential μ describes N interacting electrons and can be written as $\hat{H} = \hat{H}_{SO(4)} - \mu[N_a - \hat{N}]$, where $\hat{H}_{SO(4)} = \hat{T} + U[\hat{D} - \hat{N}/2]$, $\hat{T} = -t_a \sum_{j,\sigma}[c_{j\sigma}^{\dagger} c_{j+1\sigma} + h.c.]$ is the "kinetic energy", $\hat{D} = \sum_j \hat{n}_{j,\uparrow}\hat{n}_{j,\downarrow}$ measures the number of doubly occupied sites, $\hat{N} = \sum_{j,\sigma} \hat{n}_{j,\sigma}$, $c_{j\sigma}^{\dagger}$ and $c_{j\sigma}$ are electron operators of spin projection σ at site $j = 1, ..., N_a$, and $\hat{n}_{j,\sigma} = c_{j\sigma}^{\dagger} c_{j\sigma}$. We choose a density $n = N/N_a$ in the interval $0 \leq n \leq 1$ with even N and zero magnetization and define $k_F = \pi n/2$. We use units such that $-e = \hbar = 1$, where $-e$ is the electronic charge. The conductivity can be written as

$$\sigma_1^{reg}(\omega) = \frac{\pi}{N_a} \sum_{\nu \neq 0} \frac{|\langle \nu | \hat{J} | 0 \rangle|^2}{\omega_{\nu,0}} \delta(\omega - \omega_{\nu,0}) \, , \tag{1}$$

and is also given by $\sigma_1^{reg}(\omega) \propto \lim_{k \rightarrow 0} \frac{\omega Im \chi_\rho(k,\omega)}{k^2}$, where $\hat{J} = -it_a \sum_{j,\sigma} \left[c_{j\sigma}^{\dagger} c_{j+1\sigma} - c_{j+1\sigma}^{\dagger} c_{j\sigma} \right]$ is the current operator, the summation runs over energy eigenstates, $\omega_{\nu,0} = E_\nu - E_0$ is the excitation energy, $\chi_\rho(k,\omega) = -\sum_{\nu \neq 0} \frac{|\langle \nu | \hat{n}(k) | 0 \rangle|^2 \, 2\omega_{\nu,0}}{\omega_{\nu,0}^2 - (\omega + i\delta)^2}$ is the charge-charge response function, and $\hat{n}(k) = \sum_{k',\sigma} c_{k'+k,\sigma}^{\dagger} c_{k',\sigma}$. The formula (1) applies if the GS $|0\rangle$ is non-degenerate. This is true for an even number of sites N_a if periodic (anti-periodic) boundary conditions are used for odd (even) values of $\frac{N}{2}$, respectively. The GS is then necessarily an eigenstate of the parity operator, $\hat{P}_\pi$, which moves electrons from sites j to $N_a + 1 - j$, $j = 1, ..., N_a$, and has

eigenvalues ± 1. Importantly, in the present model $\hat{P}_\pi$ commutes with the Hamiltonian and anticommutes with the current operator. This implies immediately that the states $|0\rangle$ and $\hat{J}|0\rangle$ have opposite parities, a *key selection rule* for optical transitions. The final states $|\nu\rangle$ can be characterized in terms of holons, antiholons, spinons [12,13], and a charge-transfer band (CTB) [14]. The holon/antiholon and spinon bands describe low-energy charge and spin excitations, whereas the CTB is associated with the upper Hubbard band [3]. We use the labels $\alpha = c, s, t$ for the holon/antiholon band, the spinon band, and the CTB, respectively [14], and the quantum number β for distinguishing between holons ($\beta = -\frac{1}{2}$) and antiholons ($\beta = +\frac{1}{2}$) [13,14]. In the present context, the excitations that couple to the GS are such that the s band is empty of spinons, the c band can be populated by holons and by zero or one antiholon, and the t band can have occupancy zero or one. The momentum variable has the form $q_j = \frac{2\pi}{N_a} I_j^\alpha$, where I_j^α are successive integers or half-odd integers. In contrast to the case of electronic bands, the number of available momenta N_α^* can change with band occupancies. These numbers are $N_c^* = N_a$, $N_s^* = N/2 - N_t$, and $N_t^* = N_a - N + N_t$, where N_t is the number of occupied momenta in the CTB, and the momentum band widths are $\Delta q_c = 2\pi$, $\Delta q_s = 2k_F - 2\pi N_t/N_a$, and $\Delta q_t = 2\pi - 4k_F + 2\pi N_t/N_a$. The numbers $N^h_{c,-\frac{1}{2}}$ (holons), $N^h_{c,+\frac{1}{2}}$ (antiholons), and N_t are good quantum numbers which obey the sum rules [14], $N_a - N = -2\sum_{\beta=\pm\frac{1}{2}} \beta N^h_{c,\beta} = N_c^h - 2N_t$, where $N_c^h = \sum_{\beta=\pm\frac{1}{2}} N^h_{c,\beta}$. The GS is characterized by $N^h_{c,+\frac{1}{2}} = N_t = 0$ and $N^h_{c,-\frac{1}{2}} = N_a - N$, with a symmetrical holon occupancy in the c band for momenta $2k_F < |q| < \pi$. The GS α pseudo-Fermi momenta read $q_{F\alpha} = \pi N_\alpha/N_a$ where $N_\alpha = N_\alpha^* - N_\alpha^h$ and thus $q_{Fc} = 2k_F$, $q_{Fs} = k_F$, and $q_{Ft} = 0$. The energy bands $\epsilon^0_\alpha(q)$ are defined by Eqs. (110)-(112) and (C7)-(C9) of Ref. [14]. [See also Figs. 7 and 8 of Ref. [15] for $\epsilon_\alpha(q) = \epsilon^0_\alpha(q) - \epsilon^0_\alpha(q_{F\alpha})$ and $\alpha = c, s$.] The velocities $v_\alpha(q) = d\epsilon^0_\alpha(q)/dq$ and $v_\alpha \equiv v_\alpha(q_{F\alpha})$ and the mass $1/m^*_\alpha \equiv |dv_\alpha(q)/dq|_{q=q_{F\alpha}}$ are also important quantities. In the parameter region of appreciable oscillator strength for optical transitions, which corresponds to $n = 1$ and to densities close to $n = 1$ for large enough (but not too large) values of U [3], the CTB width $W_t = \epsilon^0_t(0) - \epsilon^0_t(\pi - 2k_F) = \epsilon^0_t(0)$ either vanishes ($n = 1$) or is very small. There is

nearly no oscillator strength for $U < U^*$, where $U^* = U^*(n)$ is such that $E_c(n, U^*) = 0$. Here $E_c(n, U) = E_c \equiv -2\epsilon_c^0(\pi)$ and $E_c > 0$ (and $E_c < 0$) for $U > U^*$ ($U < U^*$) and $E_c \to U - 4t$ ($E_c \to E_{MH}$) as $n \to 0$ ($n \to 1$). (E_{MH} is the $n = 1$ Mott-Hubbard gap [14].) U^* is a decreasing function of n given by $U^* = 0$ ($U^* = 4t$) for $n \to 1$ ($n \to 0$).

The main transitions contributing to $\sigma_1^{reg}(\omega)$ are of two types: (a) those leaving the band filling $N^h_{c,-\frac{1}{2}}$, $N^h_{c,+\frac{1}{2}}$, and N_t unchanged and (b) those changing these numbers by $\Delta N^h_{c,-\frac{1}{2}} = \Delta N^h_{c,+\frac{1}{2}} = \Delta N_t = 1$. The former start, in principle, at $\omega = 0$, while the latter have an onset at $E_{opt} = W_t - 2\epsilon_c^0(2k_F) > 0$. We find below that for $n \neq 1$ (or $n = 1$) E_{opt} is a pseudogap (or a gap). Importantly, for $\omega < E_{opt}$ the final-state Hilbert subspace is spanned by states with no occupancy in the t band. In this case the excitations are described by holons and spinons and at low values of ω and $n \neq 1$ the quantum liquid is a TLL. On the other hand, for $\omega > E_{opt}$ the final-state subspace is spanned by states also involving t occupation, the charge and spin excitations remaining separated and described by holons and spinons. For $n \neq 1$ this c, s, and t quantum liquid describes the DMHL. The collisions involving holons, antiholons, spinons, and t particles do not lead to energy and momentum transfer and only give rise to shifts in the phases of these elementary particles. We find below that for both the TLL and DMHL the critical exponent expressions are simply a linear superposition of the phase-shift parameters $\xi^j_{\alpha\alpha'} = \delta_{\alpha,\alpha'} + \sum_{l=\pm 1} l^j \Phi_{\alpha\alpha'}(q_{F\alpha}, l q_{F\alpha'})$ with $j = 0, 1$. Here $\Phi_{\alpha\alpha'}(q, q')$ are the two-particle forward-scattering phase shifts defined by Eqs. (103) and (B30)-(B38) of Ref. [14]. For holons and spinons the 8 parameters $\xi^j_{\alpha\alpha'}$ read $\xi^1_{cc} = 2\xi^1_{cs} = 1/\xi^0_{cc} = \sqrt{2K_\rho}$, $\xi^1_{ss} = -\xi^0_{sc} = 1/\xi^0_{ss} = 1/\sqrt{2}$, and $\xi^1_{sc} = \xi^0_{cs} = 0$ where K_ρ is the TLL parameter defined in Ref. [3] and $\xi^1_{\alpha\alpha'}$ are the entries of the transverse of the conformal-field theory (CFT) dressed-charge matrix [16]. The TLL critical expressions involve v_c, v_s, and K_ρ [3]. On the other hand, the low-energy $(\omega - E_{opt}) > 0$ DMHL critical theory (above the pseudogap) is a three-component quantum liquid of the general type studied in Ref. [9] and involves v_c, v_s, m_t^*, and the 18 parameters $\xi^j_{\alpha\alpha'}$. Importantly, some of these parameters are n and U dependent and cannot be expressed in terms of the TLL quantity K_ρ. (The $n = 1$ and $(\omega - E_{MH}) > 0$ critical theory is also of that type and involves v_s, m_c^*, and m_t^*.)

The transitions of type (a) do not exist at $n = 1$ and we show first that, as a consequence of the selection rule presented above, they have a very small weight for $n < 1$. These are excitations within the holon band which can be characterized in terms of single and multiple electron-hole excitations [17]. Single electron-hole excitations give no contributions to the finite-frequency absorption, while multiple excitations are expected to decrease very rapidly in intensity. For low ω we evaluate $\sigma_1^{reg}(\omega)$ from $\chi_\rho(k,\omega) \propto \int dx \int dt e^{i[kx-\omega t]} \chi_\rho(x,t)$, with the charge-charge correlation function $\chi_\rho(x,t)$ obtained directly from CFT [16]. Double excitations, which would give a contribution $\sigma_1(\omega) = C_3\,\omega^3$, are forbidden by the parity selection rule and thus $C_3 = 0$, since these transitions require symmetrical changes of holon occupancies at q and $-q$, leaving the parity unchanged. This explains why the ω^3 absorption was not observed in optical experiments [2]. Higher-order low-energy processes would give rise to $\sigma_1(\omega) = C_7\,\omega^7$ for $n \neq 1$ and to $\sigma_1(\omega) = A_j\,\omega^{4j^2K_\rho - 1}$ for $n = 1/j$ with $j = 2, 3, 4...$ (due to *Umklapp* processes). [These two exact low-ω CFT expressions can be obtained by multiplying the perturbative expressions ω^3 and $\omega^{4j^2K_\rho-5}$, respectively, of Ref. [10] by the factor ω^4, which is missing in the latter two expressions.] Since these processes require multiple excitations in the holon band, they have extremely low spectral weight and $C_7\,, A_j \approx 0$. These considerations explain why numerical studies yield so weak features at low frequencies [7]. While in 1D the $\hat{P}_\pi$ eigenvalues ± 1 are directly related to the right and left state occupancies and the selection rule is very restrictive, at higher dimensions it is less effective because there are many angular-momentum channels which lead to significant spectral weight at small values of ω [11]. The weakness of type (a) transitions implies that the onset of type (b) transitions at E_{opt} represents a pseudogap which for $n < 1$ and $U > U^*$ looks like a true gap in an actual experiment [1,2]. E_{opt}, shown in Fig. 1 (a), increases with increasing U and decreases with increasing density. For $n = 1$ it coincides with the Mott-Hubbard gap, $E_{MH} = E_c(1, U)$. Since larger interchain transfer integral t_b means larger effective doping for the single chains, this theoretical result is fully consistent with the experimental data of Fig. 3 of Ref. [1]. The important processes for the type (b) transitions are those where in addition to a particle at q' in the t band a holon-antiholon pair is created in the c band at

q and $q'-q$ (with $q'=0$ for $n=1$). This leads to final states whose excitation energy has its minimum and maximum values at $\omega = E_{opt}$ and $\omega = E_{opt} + \Delta\omega_{opt}$, respectively. Here $\Delta\omega_{opt} = 8t_a - 2\epsilon_F^h$ where $\epsilon_F^h = \epsilon_c^0(\pi) - \epsilon_c^0(2k_F) = 0$ at $n=1$. This spectral range agrees with large U expansions [4] and numerical calculations [5,7]. For $n=1$ there are only these final states and for $n<1$ the missing multipair processes contain nearly no spectral weight. The current operator cannot produce more than one doubly occupied site. Since from the results of Refs. [14,17] we find that creating one t particle involves processes which create one of these sites, there will be almost no spectral weight above the upper edge at $\omega = E_{opt} + \Delta\omega_{opt}$.

The evaluation of the line shape is a very difficult problem. We could solve it both for $n \leq 1$ and the region immediately above threshold and for $n=1$ and energies immediately below the top absorption edge. Since the number operators $\hat{N}_\alpha$ are conservation laws [8] and the t band is quadratic for small q, the low-energy spectrum of the *Conservation-Laws Hamiltonian*, $\hat{H}_{CL} \equiv \hat{H}_{SO(4)} - \sum_\alpha \epsilon_\alpha^0(q_{F\alpha})\hat{N}_\alpha - \mu N_a$, is of the type studied in Ref. [9]. The use of the non-linear band approach of that reference allows the evaluation of asymptotic expressions for the charge-charge correlation function of $\hat{H}_{CL}$, $\chi_\rho^{CL}(x,t)$. However, that approach *does not* provide finite-energy correlation-function expressions. Fortunately, the following symmetries and properties of $\hat{H}$ and $\hat{H}_{CL}$ allow solution of this problem [8]: (i) the leading term in $\chi_\rho^{CL}(x,t)$ has contributions only from transitions to a Hilbert subspace with fixed N_α numbers; (ii) $[\hat{H}, \hat{H}_{CL}] = 0$, and thus $\hat{H}$ and $\hat{H}_{CL}$ have the same eigenstates; and (iii) for the final subspace relevant to the conductivity, the difference in energies is $E_{opt} = \langle\psi|\hat{H}|\psi\rangle - \langle\psi|\hat{H}_{CL}|\psi\rangle$ and is *the same for all final states* $|\psi\rangle$ in that subspace. Using these results, we can show that the corresponding leading term in the Hubbard model correlation function is of the form $\chi_\rho(x,t) = e^{iE_{opt}t}\chi_\rho^{CL}(x,t)$. This provides $\chi_\rho(k,\omega) = \int dx \int dt e^{i[kx-(\omega-E_{opt})t]}\chi_\rho^{CL}(x,t)$ for small values of both k and $(\omega - E_{opt}) > 0$ which for $n<1$ leads to $\sigma_1^{reg}(\omega) = C\Big(\frac{[\omega-E_{opt}]}{E_{opt}}\Big)^\zeta$ at the onset and a critical exponent $\zeta = -\frac{3}{2} + \frac{1}{2}\Big(\sqrt{\frac{2}{K_\rho}} - \xi_{ct}^0\Big)^2 + \frac{1}{2}\Big(\xi_{st}^0\Big)^2$. As expected, this DMHL exponent cannot be expressed in terms of the TLL parameter K_ρ only. It is shown in Fig. 1 (b) and approaches $\frac{1}{2}$ both as $n \to 1$ at finite U and as $U \to \infty$, and it increases with decreasing values of U. C increases with

increasing n and for $U < U^*$ is vanishing small. Consistently with the $n < 1$ results, at $n = 1$ we find $\sigma_1^{reg}(\omega) = C\Big(\frac{[\omega - E_{MH}]}{E_{MH}}\Big)^{1/2}$ for all finite values of U, in contrast to the naive $\Big(\omega - E_{MH}\Big)^{-1/2}$ prediction of Ref. [10]. At $n = 1$ we could also find that $\sigma_1^{reg}(\omega)$ has a maximum at $\omega = \omega_0$ with $E_{MH} < \omega_0 \leq E_{MH} + 4t_a$ and $\omega_0 \rightarrow E_{MH} + 4t_a$ as $U \rightarrow \infty$, and that for energies immediately below the top conductivity edge at $E_{MH} + 8t_a$, $\sigma_1^{reg}(\omega)$ reads $\sigma_1^{reg}(\omega) = C'\Big(\frac{[E_{MH} + 8t_a - \omega]}{E_{MH}}\Big)^{1/2}$. At U large the ratio C'/C equals one and the conductivity absorption is symmetric around $\omega = \omega_0 = E_{MH} + 4t_a \approx U$, in agreement with the results of Refs. [4,6]. However, C'/C decreases with decreasing U and ω_0 is shifted to lower values of ω. In this case $\sigma_1(\omega)$ is not symmetric around ω_0 and a dependence $\sigma_1(\omega) \propto \omega^{-\gamma}$ is expected for a conductivity descending region of intermediate ω values of the domain $\omega \in (\omega_0\,, E_{opt} + 8t_a)$. (In contrast to the onset exponent ζ, γ cannot be calculated within our critical theory and the use of TLL [2,10] to estimate it is an open question.)

The $X = ClO_4$ and $T = 10K$ curves of Figs. 1 (B) of Ref. [1] and Figs. 3 and 4 of Ref. [2] correspond to a $\omega = 0$ Drude peak with a very small carrier density separated by a pseudogap $E_{opt} \approx 0.014\,eV$ from an absorption band with $\gamma \approx 1.3$ and a width $\Delta\omega_{opt} \approx 1.00\,eV$. These E_{opt} and $\Delta\omega_{opt}$ values can be understood in the framework of the 1D Hubbard model with effective values $t_a \approx 0.125\,eV$ [tight-binding model (TBM) calculations [1,2] lead to $t_a \approx 0.250\,eV$ because the energy width of the $\epsilon_c(q)$ band GS occupancy, $4t_a - \epsilon_F^h$, is about twice that of the TBM band] and $U/t_a \approx 1.5$ if the system has a nearly half-filled band, $n \approx 0.995$, in which case the optical threshold $E_{opt} \approx E_{MH} \approx 0.11\,t_a \approx 0.014\,eV$ and $\Delta\omega_{opt} \approx 8t_a \approx 1.00\,eV$. Moreover, combining the theoretical values for $\Delta\omega_{opt} \approx 8t_a$ and the sumrule $\int_{-\infty}^{\infty} \sigma_1(\omega)$ [3], we find $C \approx 1.2\,\sigma_1^{reg}(\omega_0) \approx 3600\,\Omega^{-1}cm^{-1}$. A crucial text for our theoretical description is whether the exponent ζ obtained from the observed sharp onset of absorption [1,2] agrees with the t_a, U, and n values extracted from E_{opt} and $\Delta\omega_{opt}$. Except for the small onset temperature tail, we find from the above figures the linear behavior, $\ln\Big(\frac{\sigma_1^{reg}(\omega)}{\sigma_1^{reg}(\omega_0)}\Big) \approx \zeta\,\ln\Big(\frac{[\omega - E_{opt}]}{E_{opt}}\Big) + \ln(\frac{C}{\sigma_1^{reg}(\omega_0)})$ for $\frac{[\omega - E_{opt}]}{E_{opt}} < 0.5$, where $\zeta \approx 0.65$ and $C \approx 3530\,\Omega^{-1}cm^{-1}$. The corresponding asymptotic theoretical conductivity curve is plotted in Fig. 2. Importantly, Fig. 1 (b) reveals that this exponent is consistent with the above U/t_a and n values.

We thank D. Baeriswyl, D.K. Campbell, E. Dagotto, T. Giamarchi, P. Horsch, and J.M.B. Lopes dos Santos for illuminating discussions. This research was supported by the Department of Energy under contract W-7405-ENG-36 and by PRAXIS under Grant No. 2/2.1/FIS/302/94.

REFERENCES

[1] V. Vescoli *et al.*, Science **281**, 1181 (1998).

[2] A. Schwartz *et al.*, Phys. Rev. B **58**, 1261 (1998).

[3] H. Schulz, Phys. Rev. Lett. **64**, 2831 (1990); Henk Eskes and Andrzej M. Oleś, *ibid.* **73**, 1279 (1994).

[4] F. Gebhard, Philos. Mag. B **75**, 47 (1997).

[5] E. Y. Loh, JR. and D. K. Campbell, Synth. Metals **27**, A499 (1988).

[6] F. B. Gallagher and S. Mazumdar, Phys. Rev. B **56**, 15 025 (1997).

[7] W. Stephan and P. Horsch, Phys. Rev. B **42**, 8736 (1990); R. M. Fye, M. J. Martins, D. J. Scalapino, J. Wagner, and W. Hanke, Phys. Rev. B **44**, 6909 (1991).

[8] J. M. P. Carmelo, L. M. Martelo, T. Prosen, and D. K. Campbell, unpublished.

[9] J. M. P. Carmelo, J. M. E. Guerra, J. M. B. Lopes dos Santos, and A. H. Castro Neto, Phys. Rev. Lett. **83**, 3892 (1999).

[10] T. Giamarchi, Physica B **230-232**, 975 (1997), and references therein.

[11] E. Dagotto, A. Moreo, F. Ortolani, D. Poilblanc, and J. Riera, Phys. Rev. B **45**, 10 741 (1992).

[12] F. H. L. Essler and V. E. Korepin, Phys. Rev. Lett. **72**, 908 (1994).

[13] J. M. P. Carmelo and N. M. R. Peres, Nucl. Phys. B **458**, 579 (1996).

[14] For the relation to the Bethe-ansatz solution, see J. M. P. Carmelo and N. M. R. Peres, Phys. Rev. B **56**, 3717 (1997). In the present case of zero external magnetic field, the pseudoparticles described therein have simple interpretation as follows: the holons and antiholons occupy the $c, 0$ band and are the $\beta = -\frac{1}{2}$ and $\beta = +\frac{1}{2}$ pseudoholes, respectively, whereas the t particles of the charge transfer band are the $c, 1$ pseudoparticles. Their

energies, $\epsilon^0_\alpha(q)$, and phase shifts, $\Phi_{\alpha\alpha'}(q,q')$, are defined by considering $c \equiv c,0$, $s \equiv s,0$, and $t \equiv c,1$ and using the expressions of that reference.

[15] J. M. P. Carmelo and P. Horsch, P. A. Bares, and A. A. Ovchinnikov, Phys. Rev. B **44**, 9967 (1991).

[16] H. Frahm and V. E. Korepin, Phys. Rev. B **42**, 10 553 (1990).

[17] J. M. P. Carmelo and A. H. Castro Neto, Phys. Rev. B **54**, 11 230 (1996).

FIGURES

FIG. 1. (a) The pseudogap E_{opt} in units of t_a and (b) the exponent ζ as function of n for different values of U. The solid (dashed) lines correspond to $U > U^*$ ($U < U^*$).

FIG. 2. The conductivity $\sigma_1^{reg}(\omega)$ of $(TMTSF)_2ClO_4$ for $T = 10K$ as a function of $[\omega - E_{opt}]/E_{opt} > 0$ [from Fig. 4 of Ref. [2]] and the theoretical asymptotic curve $C\Big([\omega - E_{opt}]/E_{opt}\Big)^{\zeta}$ (solid line) with $\zeta = 0.65$ and $C = 3530\,\Omega^{-1}cm^{-1}$.

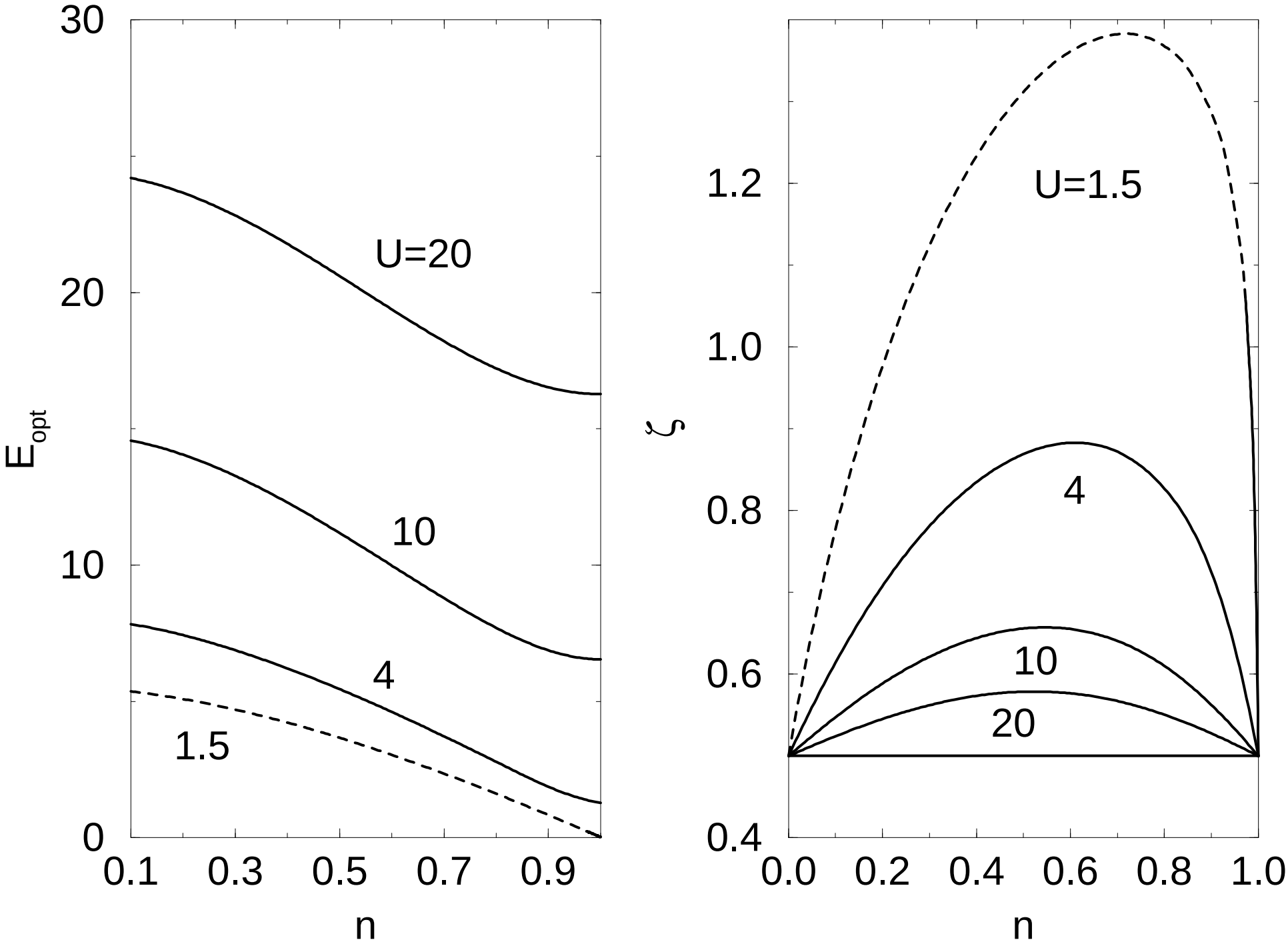
30
20
10
0
E_{opt}
U=20
10
4
1.5
0.1
0.3
0.5
0.7
0.9
n
1.2
1.0
0.8
0.6
0.4
ζ
U=1.5
4
10
20
0.0
0.2
0.4
0.6
0.8
1.0
n

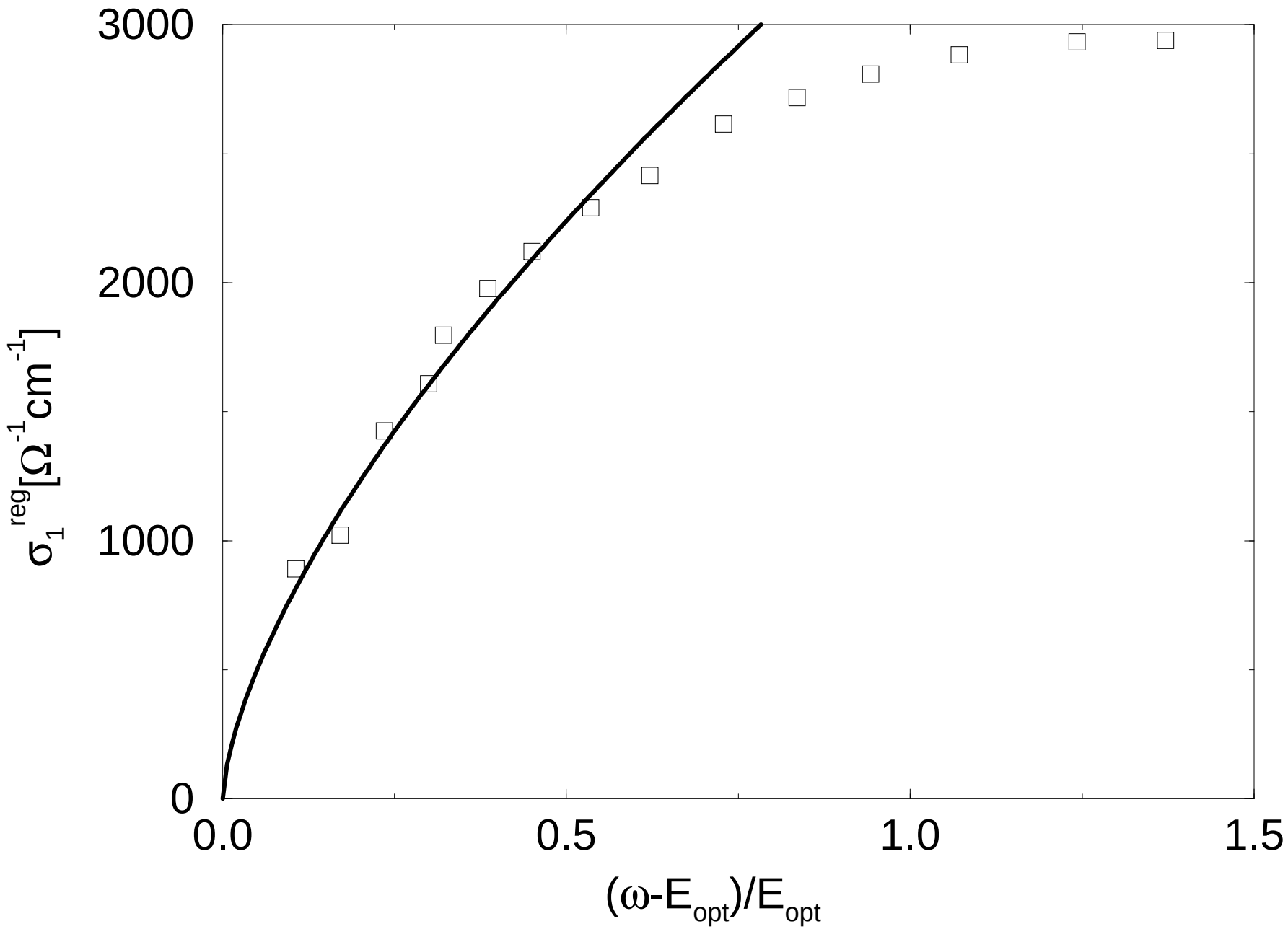
3000
2000
1000
0
0.0
0.5
1.0
1.5
$\sigma_1^{reg}[\Omega^{-1}cm^{-1}]$
$(\omega-E_{opt})/E_{opt}$